

# Lattice Boltzmann simulations of anisotropic particles at liquid interfaces

F. Günther\*, F. Janoschek\*, S. Frijters\*, and J. Harting\*,\*\*

Corresponding author: j.harting@tue.nl

\* Department of Applied Physics, Eindhoven University of Technology, The Netherlands.

\*\* Institute for Computational Physics, University of Stuttgart, Germany.

---

---

**Abstract:** Complex colloidal fluids, such as emulsions stabilized by particles with complex shapes, play an important role in many industrial applications. However, understanding their physics requires a study at sufficiently large length scales while still resolving the microscopic structure of a large number of particles and of the local hydrodynamics. Due to its high degree of locality, the lattice Boltzmann method, when combined with a molecular dynamics solver and parallelized on modern supercomputers, provides a tool that allows such studies. Still, running simulations on hundreds of thousands of cores is not trivial. We report on our practical experiences when employing large fractions of an IBM Blue Gene/P system for our simulations. Then, we extend our model for spherical particles in multicomponent flows to anisotropic ellipsoidal objects rendering the shape of e.g. clay particles. The model is applied to a number of test cases including the adsorption of single particles at fluid interfaces and the formation and stabilization of Pickering emulsions or bijels.

*Keywords:* Complex Colloidal Fluid, Lattice Boltzmann method, Blue Gene/P, Domain Decomposition, Parallelization, Ellipsoid.

## 1. Introduction

Colloidal particles are highly attractive in the food, cosmetics, and medical industries to stabilize emulsions or to develop sophisticated ways to deliver drugs at the right position in the human body. The underlying microscopic processes of emulsion stabilization with particles can be explained by assuming an oil-water mixture. Without additives, both liquids phase separate, but the mixture can be stabilized by adding small particles which diffuse to the interface and stabilize it due to a reduced interfacial free energy. If for example individual droplets of one phase are covered by particles, such systems are referred to as “Pickering emulsions”, which have been known since the beginning of the 20th century [1, 2]. Particularly interesting properties of such emulsions are the blocking of Ostwald ripening and the rheological properties due to irreversible particle adsorption at interfaces or interface bridging due to particle monolayers [3]. Recently, interest in particle-stabilized emulsions has led to the discovery of a new material type, the “bicontinuous interfacially jammed emulsion gel” (bijel), which shows an interface between two continuous fluid phases that is covered by particles. The existence of the bijel was predicted in 2005 by Stratford et al. [4] and experimentally confirmed by Herzog et al. in 2007 [5].

Computer simulations are promising to understand the dynamic properties of particle-stabilized multiphase flows. However, the shortcomings of traditional simulation methods quickly become obvious: a suitable simulation algorithm is not only required to deal with simple fluid dynamics but has to be able to simulate several fluid species while also considering the motion of the particles and the fluid-particle interactions. Some recent approaches trying to solve these problems utilize the lattice Boltzmann method

for the description of the solvents [6]. The lattice Boltzmann method can be seen as an alternative to conventional Navier-Stokes solvers and is well-established in the literature. It is attractive for the current application since a number of multiphase and multicomponent models exist which are comparably straightforward to implement. In addition, boundary conditions have been developed to simulate suspended finite-size particles in flow. These are commonly used to study the behavior of particle-laden single phase flows [7]. A few groups combined multiphase lattice Boltzmann solvers with the known algorithms for suspended particles [4, 8]. In this paper we follow an alternative approach based on the multicomponent lattice Boltzmann model of Shan and Chen [9] which allows the simulation of multiple fluid components with surface tension. Our model generally allows arbitrary movements and rotations of rigid particles of arbitrary shape. Further, it allows an arbitrary choice of the particle wettability – one of the most important parameters for the dynamics of multiphase suspensions [3]. For a detailed introduction to the method see Ref. [10], where our model has been applied to spherical particles at fluid interfaces. We have presented a thorough validation of the method for single particle situations and have shown that a transition from a bijel to a Pickering emulsion can be found by varying the particle concentration, the particle’s contact angle, or the volume ratio of the solvents. Further, we investigated the temporal evolution of the droplet/domain growth in emerging Pickering emulsions and bijels.

Modelling colloidal particles as perfect spheres is a strong simplification of systems appearing in nature. There, the particles are generally not spherical, but might show geometrical distortions or fully anisotropic shapes, as is, for example, common for clay particles. As a first step to investigate the impact of particle anisotropy on the adsorption and stabilization properties, this paper focuses on ellipsoidal particles. In addition to the properties of spheres adsorbed at an interface, in the case of anisotropic ellipsoidal particles the orientation becomes important and the process of adsorption is in this case more complex [11]. Furthermore the anisotropy of the ellipsoids leads in general to a deformation of the interface. However, an adsorbed sphere or ellipsoid with a contact angle  $\theta = 90^\circ$  does not deform the interface in absence of an external potential such as gravitation. For multiple particles capillary interactions, which depend on the distance and the orientation of the particles, become relevant [12] and orientational discontinuous phase transitions of the particles can be found [13]. Experimentally it was shown that the number of ellipsoidal particles required to stabilize a fluid-fluid interface decreases with increasing particle aspect ratio and that a tip-to-tip arrangement is dominant [14].

The remaining sections are organized as follows: In section 2 the simulation method (lattice Boltzmann combined with molecular dynamics) is illustrated. Since studying particle-stabilized emulsions demands an exceptional amount of computing resources we focus on specific implementation details of our simulation code in section 3. In particular, we highlight specifically code improvements that allow to harness the power of massively parallel supercomputers, such as the Blue Gene/P system JUGENE at Jülich Supercomputing Centre with its ability to run up to 294912 MPI (Message Passing Interface) tasks in parallel. The following section reports on simulations of single particle adsorption of ellipsoidal particles and the formation of bijels and Pickering emulsions. Finally, we conclude in section 5.

## 2. Simulation method

The lattice Boltzmann method is a very successful tool for modelling fluids in science and engineering. Compared to traditional Navier-Stokes solvers, the method allows an easy implementation of complex boundary conditions and—due to the high degree of locality of the algorithm—is well suited for the implementation on parallel supercomputers. For a thorough introduction to the lattice Boltzmann method we refer to Ref. [6]. The method is based on a discretized version of the Boltzmann equation

$$f_i^c(\mathbf{x} + \mathbf{c}_i, t + 1) = f_i^c(\mathbf{x}, t) + \Omega_i^c(\mathbf{x}, t), \quad (1)$$

where  $f_i^c(\mathbf{x}, t)$  is the single-particle distribution function for fluid component  $c$  after discretization in space  $\mathbf{x}$  and time  $t$  with a discrete set of lattice velocities  $\mathbf{c}_i$  and

$$\Omega_i^c(\mathbf{x}, t) = -\frac{f_i^c(\mathbf{x}, t) - f_i^{\text{eq}}(\rho^c(\mathbf{x}, t), \mathbf{u}^c(\mathbf{x}, t))}{\tau} \quad (2)$$

is the Bhatnagar-Gross-Krook (BGK) collision operator.  $f_i^{\text{eq}}(\rho^c, \mathbf{u}^c)$  is the equilibrium distribution function and  $\tau$  is the relaxation time. We use a three-dimensional lattice and a D3Q19 implementation ( $i = 1, \dots, 19$ ). From Eq. (1), the Navier-Stokes equations can be recovered with density  $\rho^c(\mathbf{x}, t) = \sum_i f_i^c(\mathbf{x}, t)$  and velocity  $\mathbf{u}^c = \sum_i f_i^c \mathbf{c}_i / \rho^c$  in the low-compressibility and low Mach number limit. If further fluid species  $c'$  with a single-particle distribution function  $f_i^{c'}(\mathbf{x}, t)$  are to be modeled, the inter-species interaction force

$$\mathbf{F}^c(\mathbf{x}, t) = -\Psi^c(\mathbf{x}, t) \sum_{c'} g_{cc'} \sum_{\mathbf{x}'} \Psi^{c'}(\mathbf{x}', t) (\mathbf{x}' - \mathbf{x}), \quad (3)$$

with a monotonous weight function  $\Psi^c(\mathbf{x}, t)$  for the effective mass is calculated locally according to the approach by Shan and Chen and incorporated into the collision term  $\Omega_i^c$  in Eq. (1) [9]. In our case, the coupling strength  $g_{cc'}$  is negative in order to obtain de-mixing and the sum over  $\mathbf{x}'$  runs over all sites separated from  $\mathbf{x}$  by one of the discrete  $\mathbf{c}_i$ . Colloidal particles are discretized on the lattice and coupled to both fluid species by means of a moving bounce-back boundary condition [15, 7]: if  $\mathbf{x}$  is part of the surface of a colloid then Eq. (1) for adjacent fluid sites  $\mathbf{x} + \mathbf{c}_i$  is replaced with

$$f_i^c(\mathbf{x} + \mathbf{c}_i, t + 1) = f_i^c(\mathbf{x} + \mathbf{c}_i, t) + \Omega_i^c(\mathbf{x} + \mathbf{c}_i, t) + C, \quad (4)$$

where  $C = \frac{2\alpha_{c_i}}{c_s^2} \rho^c(\mathbf{x} + \mathbf{c}_i, t) \mathbf{u}_{\text{surf}} \cdot \mathbf{c}_i$  is a linear function of the local particle surface velocity  $\mathbf{u}_{\text{surf}}$  and the direction  $\bar{i}$  is defined via  $\mathbf{c}_i = -\mathbf{c}_{\bar{i}}$ .  $\alpha_{c_i}$  and  $c_s$  are constants of the D3Q19 lattice. The particle configuration is evolved in time solving Newton's equation in the spirit of classical molecular dynamics simulations. As the total momentum should be conserved, an additional force

$$\mathbf{F}(t) = (2f_{\bar{i}}^c(\mathbf{x} + \mathbf{c}_i, t) + C) \mathbf{c}_{\bar{i}} \quad (5)$$

acting on the particle is needed to compensate for the momentum change of the fluid caused by Eq. (4). The potential between the particles is a Hertz potential which approximates a hard core potential and has the following form for two spheres with the same radius  $R$  [16]:

$$\phi_H = K_H (2R - r_{ij})^{\frac{5}{2}} \quad \text{for } r_{ij} \leq 2R. \quad (6)$$

$r_{ij}$  is the distance between the two sphere centers and  $K_H$  the force constant. For the simulations which are discussed later in this text a value of  $K_H = 100$  is used. In the next step the potential is generalized to the case of ellipsoids with the parallel radius  $R_p$  and the orthogonal radius  $R_o$  by following the method which was applied by Berne and Pechukas for the case of an intermolecular potential [17]. We define  $\sigma = 2R$  and  $\varepsilon = K_H \sigma^{\frac{5}{2}}$  and extend  $\sigma$  and  $\varepsilon$  to the anisotropic case so that

$$\varepsilon(\hat{\mathbf{o}}_i, \hat{\mathbf{o}}_j) = \frac{\bar{\varepsilon}}{\sqrt{1 - \chi^2(\hat{\mathbf{o}}_i \hat{\mathbf{o}}_j)^2}} \quad \text{and} \quad \sigma(\hat{\mathbf{o}}_i, \hat{\mathbf{o}}_j, \hat{\mathbf{r}}_{ij}) = \frac{\bar{\sigma}}{\sqrt{1 - \frac{\chi}{2} \left( \frac{(\hat{\mathbf{r}}_{ij} \hat{\mathbf{o}}_i + \hat{\mathbf{r}}_{ij} \hat{\mathbf{o}}_j)^2}{1 + \chi \hat{\mathbf{o}}_i \hat{\mathbf{o}}_j} + \frac{(\hat{\mathbf{r}}_{ij} \hat{\mathbf{o}}_i - \hat{\mathbf{r}}_{ij} \hat{\mathbf{o}}_j)^2}{1 - \chi \hat{\mathbf{o}}_i \hat{\mathbf{o}}_j} \right)}}, \quad (7)$$

with  $\bar{\sigma} = 2R_o$ ,  $\chi = \frac{R_p^2 - R_o^2}{R_p^2 + R_o^2}$ , and  $\hat{\mathbf{o}}_i$  the orientation vector of particle  $i$ . The scaled potential can be written as

$$\phi_H(\hat{\mathbf{o}}_i, \hat{\mathbf{o}}_j, \mathbf{r}_{ij}) = \varepsilon(\hat{\mathbf{o}}_i, \hat{\mathbf{o}}_j) \tilde{\phi}_H \left( \frac{r_{ij}}{\sigma(\hat{\mathbf{o}}_i, \hat{\mathbf{o}}_j, \hat{\mathbf{r}}_{ij})} \right). \quad (8)$$

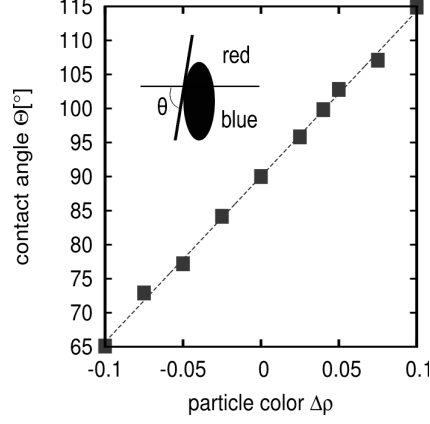


Figure 1: Relation between the particle color  $\Delta\rho$  and the contact angle  $\Theta$ . A linear relation is found:  $\Theta = 243.2^\circ\Delta\rho + 90^\circ$ . Inset: Definition of the contact angle  $\Theta$  for an ellipsoidal particle adsorbed at an interface between two fluids.

$\tilde{\Phi}_H$  is a dimensionless function which takes the specific form of the potential form into account. In addition to adding the direct interaction described by the Hertz potential we correct for the limited description of hydrodynamics when two particles come very close by means of a lubrication correction. If the number of lattice points between two particles is sufficient, the lattice Boltzmann algorithm reproduces the correct lubrication force automatically. The error that occurs if the flow is not sufficiently resolved can be corrected by

$$\mathbf{F}_{ij} = \frac{3\pi\mu R^2}{2} \hat{\mathbf{r}}_{ij} (\hat{\mathbf{r}}_{ij} (\mathbf{u}_i - \mathbf{u}_j)) \left( \frac{1}{r_{ij} - 2R} - \frac{1}{\Delta_c} \right) \quad (9)$$

in the case of two spheres with radius  $R$ . We choose a cut-off at  $\Delta_c = \frac{2}{3}$  and  $\mathbf{u}_i$  is the velocity of particle  $i$ . This equation is generalized to ellipsoids in a similar way as the Hertz potential using Eq. (7).

The force in Eq. (3) also includes interactions between lattice nodes outside of particles with a lattice node inside a particle. To calculate these interactions the lattice nodes  $\mathbf{x}$  in the outer shell of the particle are filled with fluid densities

$$\rho_{new}^c = \bar{\rho}^c = \frac{1}{N_{NP}} \sum_{i_{NP}} \rho^c(\mathbf{x} + \mathbf{c}_{i_{NP}}, t) \quad (10)$$

corresponding to the average over the  $N_{NP}$  non-particle lattice nodes adjacent to  $\mathbf{x}$  in directions  $i_{NP}$ . We consider a system of two immiscible fluids, which we call red and blue fluid, and in which particles are suspended. By defining a parameter  $\Delta\rho$ , the particle color, we are able to control the interaction between the particle surface and the two fluids and thus control the contact angle  $\Theta$  as it is defined in the inset of Fig. 1. If  $\Delta\rho$  has a positive value, we add it to the red fluid component as  $\rho_{new}^r = \bar{\rho}^r + \Delta\rho$ . Otherwise we add its absolute value to the blue fluid as  $\rho_{new}^b = \bar{\rho}^b + |\Delta\rho|$ . In Fig. 1 it is depicted that the dependence of the contact angle on the particle color can be fitted by the linear relation

$$\Theta = 243.2^\circ\Delta\rho + 90^\circ, \quad (11)$$

where the slope depends on the actual simulation parameters. For a more detailed description of our simulation algorithm the reader is referred to Ref. [10].

### 3. Implementation

Development of our simulation code LB3D started in 1999 as a parallel LB solver capable of describing systems of up to three fluid species coupled by Shan and Chen's aforementioned approach [9, 18].

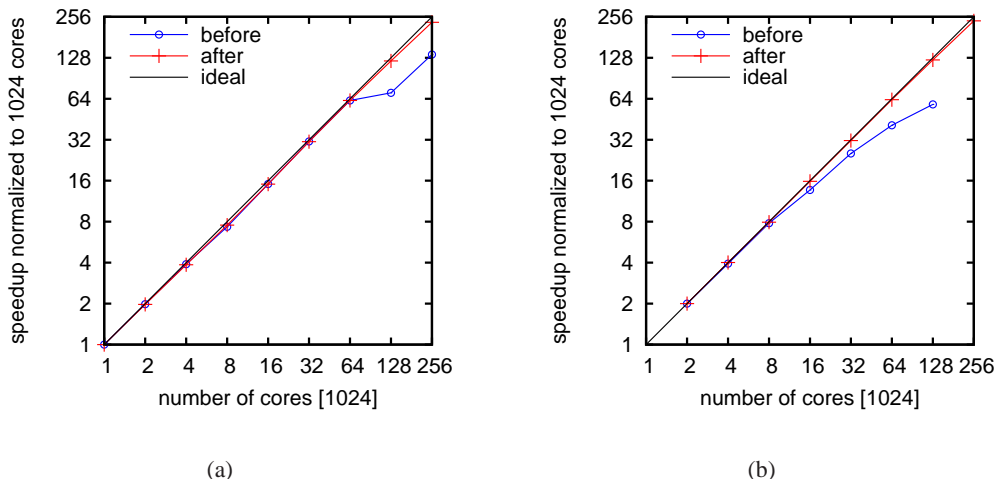


Figure 2: Strong scaling of LB3D on the Blue Gene/P before and after the optimizations. (a) relates to a system with only one fluid component so that the effect of matching or mismatching topologies of network and domain decomposition can be examined better. (b) refers to a system with two fluid species and suspended particles as they are of interest in this paper. The absolute execution times for small core counts did not change significantly.

In 2008, a—since then severely extended—parallel molecular dynamics code [19] was integrated into LB3D using a common 3-dimensional spatial decomposition scheme. It is employed here to implement the colloidal particles.

The strong locality of the LB equation Eq. (1) as well as the short-range interaction forces relevant in colloidal systems generally allow for an efficient parallelization. However, while several authors presented highly efficient combined single-component LB-suspension codes for the massively parallel simulation of blood flows on IBM Blue Gene/P systems [20, 21], it still is not trivial to achieve good scalability on this platform. For example, the network employed for MPI point-to-point communication provides direct links only between nearest neighbors in a three-dimensional torus. Allowing `MPI_Cart_create()` to reorder process ranks and manually choosing a domain decomposition that fits the known hardware topology can therefore increase the performance significantly at high degrees of parallelism. Fig. 2(a) demonstrates this on the basis of strong scaling speedup for a system of  $1024^2 \times 2048$  lattice sites carrying only one fluid species and no particles. Consequently, only Eq. (1) demands significant computational effort, which makes possible communication bottlenecks more visible. On the other hand, JUGENE, the IBM Blue Gene/P system at Jülich Supercomputing Centre, consisting of 294912 cores, brings to light serial parts of a code which would stay undetected at lower core counts. Fig. 2(b) visualizes the effect of parallelizing a loop over the global number of colloidal particles present in earlier versions of our particle-fluid coupling routines which—in this strong scaling benchmark—had a visible effect only when scaling beyond 8192 cores. The test system of  $1024^2 \times 2048$  lattice nodes contains two fluid species and 4 112 895 uniformly distributed particles of spherical shape with a radius of 5 lattice units at a volume concentration of 20% and is thus very close to the Pickering systems of interest. When running on 262 144 cores, our two-component LB-suspension solver achieves an average of  $8.97 \times 10^9$  lattice updates per second (LUPS) in total at a decomposition of  $32 \times 16^2$  LB sites per core. This corresponds to  $3.42 \times 10^4$  LUPS per core compared to  $3.66 \times 10^4$  LUPS per core for the minimum core count of 2048 or a relative parallel efficiency of 93.5%. On average, for 262 144 cores, 41.8% of the computing time is spent on the Shan-Chen force evaluation Eq. (3), followed by 29.6% for the particle-fluid coupling and 18.7% for the LB equation Eq. (1). The remaining costs are mainly caused by communication.

While the benchmarks above relate to the pure time evolution, actual production runs require check-

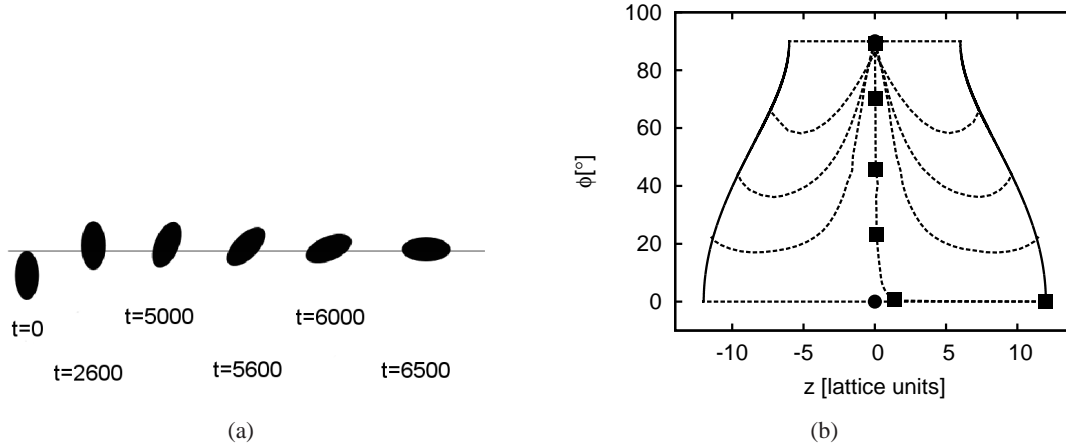


Figure 3: (a) Snapshots of the adsorption of an ellipsoid with aspect ratio  $m = 2$  and a contact angle  $\Theta = 90^\circ$  for a starting angle of  $\phi = 0.0057^\circ$ . Every snapshot is related to a square symbol in Fig. 3(b). (b) Adsorption diagram for an ellipsoid with a parallel diameter  $R_p = 12$ , an orthogonal diameter  $R_o = 6$ , and a contact angle  $\Theta = 90^\circ$ .  $z$  is the distance between the particle center and the interface,  $\phi$  is the angle between the ellipsoid main axis and the interface normal. The adsorption trajectories are presented by the dashed lines. The solid lines depict where the particle would touch an infinitely thin and undeformed interface. The circles correspond to the stable ( $\phi = \frac{\pi}{2}$ ) and the metastable ( $\phi = 0$ ) equilibrium point. The squares correspond to the snapshots in Fig. 3(a).

pointing and the output of physical observables to disk. Using parallel HDF5 output, we succeed in storing fluid density fields of 4.6GB size for a system of  $1024^2 \times 1152$  lattice sites and 454 508 particles in 29s (on average) when employing the whole system (294912 cores). This corresponds to the time required to simulate about 100 LB steps and is acceptable since output is required less than once per 100 to 1000 time steps.

Finally, it is important to be aware of possible peculiarities of the MPI implementations found on large supercomputing systems. Due to their relatively small size in memory we collect and write particle configuration data serially on the root process. When running on 131072 cores of JUGENE, we encounter a speedup of 77 when employing the specially optimized `MPI_Allgatherv()` compared to the more intuitive `MPI_Gatherv()`, at the cost of requiring one receive buffer per task.

#### 4. Results and discussion

After having discussed the implementation of our program code some of the results obtained by this program will be presented. We study a system of two immiscible fluids (called red and blue fluid in the following) stabilized by prolate ellipsoidal particles. A first step to understand fundamental physical properties of such systems is the study of the behavior of a single ellipsoidal particle at a flat fluid-fluid interface. If the particle touches the interface the particle is adsorbed to it. The binding energy of the particle is usually of the order  $10^4 k_B T$  so that the adsorption is an irreversible process. This binding energy arises from the fact that an adsorbed particle reduces the interfacial area between two fluids with repulsive interactions. The adsorption was studied in Ref. [11] using a free energy method. There, the free energy is calculated for all particle orientations and particle center-interface distances. Then, the equilibrium state is found by minimizing the free energy function. In contrast to our simulations, in the approach given in Ref. [11] the interface is infinitely thin and undeformable, while we take a finite interface thickness and a interface deformability into account.

To simulate a single-particle adsorption we use a cubic volume with a side length of 64 lattice units with two lamellae of different fluids where each lamella has a thickness of 31 lattice units. The boundary conditions are periodic in the two directions parallel to the fluid-fluid interface. Impenetrable walls are installed in the third direction at  $z = 1$  and  $z = 64$  with a thickness of 1 lattice unit each. To keep

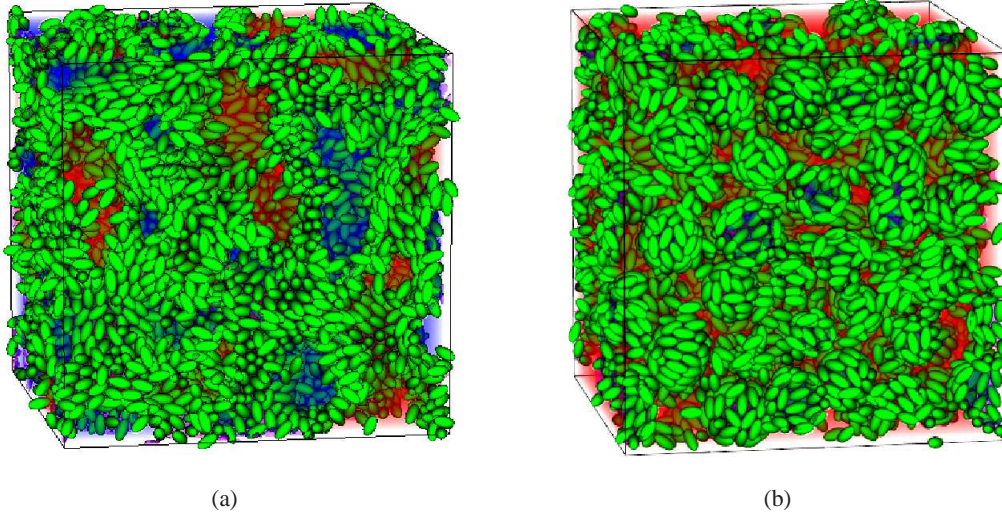


Figure 4: Two snapshots of emulsions stabilized by particles are shown for an aspect ratio  $m = 2$ , a volume concentration of  $C \approx 0.2$  and a contact angle  $\Theta = 90^\circ$ . (a) Bijel for a fluid ratio of 1 : 1. (b) Pickering emulsion for a fluid ratio of 5 : 2.

the interface thin enough the fluid-fluid interaction parameter between red and blue (Eq. (3)) is set to  $g_{br} = 0.1$ . Snapshots of the adsorption for a single ellipsoidal particle with a contact angle  $\Theta = 90^\circ$  and an aspect ratio  $m = \frac{R_p}{R_o} = 2$  are shown in Fig. 3(a) for a starting angle  $\phi = 0.0057^\circ$ .  $R_p$  and  $R_o$  are the ellipsoidal radii parallel and orthogonal to the symmetry axis. It can be observed that at the beginning of the simulation (first 2600 time steps in the present example) the particle moves in the direction of the interface without changing its orientation significantly. Thereafter ( $t = 2600 \dots 6500$  steps) the orientation changes from  $\phi \approx 0^\circ$  to  $\phi \approx 90^\circ$  and the particle reaches its equilibrium position.

Each snapshot in Fig. 3(a) is related to a square symbol in Fig. 3(b). Here,  $z$  is the distance between the particle center and the interface,  $\phi$  is the angle between the ellipsoid main axis and the interface normal. The solid lines correspond to the points where the particle just would touch an infinitely thin and undeformed interface. The dashed lines correspond to the adsorption trajectories and the two equilibria are illustrated by circles. The upper circle (at  $\phi = 90^\circ$ ) corresponds to the stable point being in relationship with the global free energy minimum whereas the lower one (at  $\phi = 0^\circ$ ) shows a metastable point. The value of the  $z$  coordinate of the stable and metastable point depends on the contact angle. In the example shown above both points have the value  $z = 0$ . If the adsorption trajectory of the particle starts with  $\phi(t = 0) = 0^\circ$  it reaches the metastable point. For any other starting angle ( $\phi(t = 0) \neq 0^\circ$ ) the adsorption trajectory of the particle ends in the stable point. The adsorption lines approach attractor lines. For initial angles much larger than  $\phi = 0^\circ$  there are two attractor lines, one on each side. The adsorption trajectories coming from the respective sides approach this attractor line. There is a third attractor line at  $z = 0$ . The adsorption trajectories starting at very small angles approach this attractor line. Qualitatively comparable theoretical calculations of the adsorption have been presented in Ref. [11]. Quantitative comparisons are not easily possible since the theoretical approach assumes an infinitely thin and undeformable interface, while our diffuse interface simulations take the interfacial deformability into account.

In the following we consider emulsions stabilized by a large number of anisotropic colloidal particles. To simulate a bulk system we use a cubic volume with a side length of 256 lattice units and periodic boundary conditions. To obtain a phase separation the fluid-fluid interaction parameter between red and blue (see Eq. (3)) is set to  $g_{br} = 0.08$ . The initial density distributions of the two fluids are chosen to be random.

As stated in the introduction we distinguish between two different phases for these emulsions, the Pickering emulsion and the bicontinuous interfacially jammed emulsion gel (bijel). The bijel [4] (see

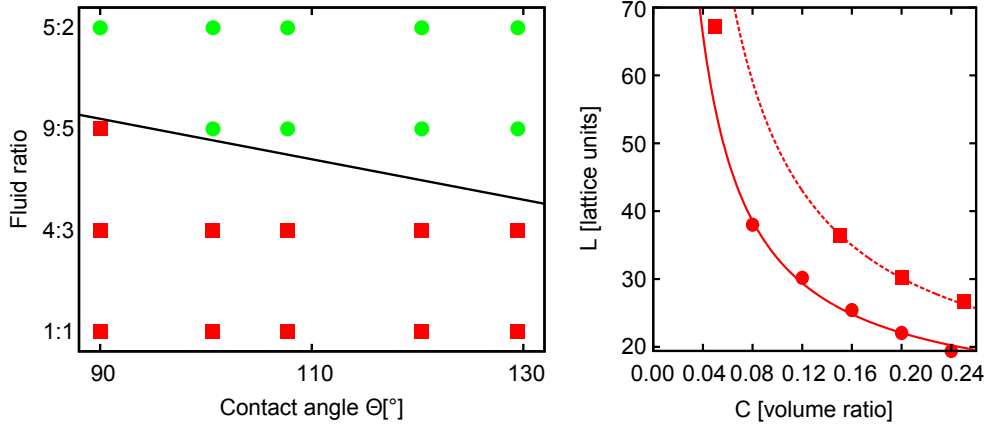


Figure 5: Left plot: Phase diagram demonstrating the transition from a bijel to a Pickering emulsion. The contact angle  $\Theta$  and the ratio between the two fluids are varied. The squares show the configurations which lead to a bijel whereas the circles denote a Pickering emulsion. Right plot: Average domain size  $L$  in equilibrium versus the volume concentration of the particles  $C$  for a bijel with particles of neutral wettability ( $\Theta = 90^\circ$ ). The plot compares the data for spheres ( $m = 1$ , cubic symbols) [10] with ellipsoids (here:  $m = 2$ , circles). The behavior can be described by  $L = \frac{a}{C} + b$  (see solid line ( $m = 2$ ) and dashed line ( $m = 1$ )), where  $a$  and  $b$  are fit parameters.

Fig. 4(a)) consists of two continuous phases whereas the Pickering emulsion [1, 2] (see Fig. 4(b)) consists of droplets of one fluid immersed in a second fluid phase. Bijels and Pickering emulsions stabilized by spherical particles have been investigated in Ref. [10]. In this paper simulation results for ellipsoids with an aspect ratio of  $m = 2$  are presented. The choice of the control parameters decides into which of the two phases the system evolves. The left plot in Fig. 5 shows the transition from a bijel to a Pickering emulsion for an aspect ratio of  $m = 2$  and a particle volume concentration of  $C \approx 0.2$ . The two control parameters used for the study of the phase transition are the fluid ratio and the contact angle  $\Theta$ . The squares show the configurations which lead to a bijel whereas the circles denote a Pickering emulsion. If the amount of the two fluids present in the simulation is equal or not too different (e.g. a ratio of 4 : 3) we find a bijel for all considered contact angles. However, if the fluid ratio is increased we find a Pickering emulsion. For intermediate fluid ratios the obtained phase depends on the chosen contact angle. For example for a ratio of 9 : 5 we get a bijel for a contact angle of  $90^\circ$  and a Pickering emulsion for all higher values of  $\Theta$ .

To characterize an emulsion the time dependent lateral domain size  $L(t) = \frac{1}{3}(L_x(t) + L_y(t) + L_z(t))$  is calculated. Its Cartesian components ( $i = x, y, z$ ) are defined as

$$L_i(t) = \frac{2\pi}{\sqrt{\langle k_i^2(t) \rangle}}, \quad \langle k_i^2(t) \rangle = \frac{\sum_{\mathbf{k}} k_i^2(t) S(\mathbf{k}, t)}{\sum_{\mathbf{k}} S(\mathbf{k}, t)}. \quad (12)$$

$\langle k_i^2(t) \rangle$  is the second-order moment of the three-dimensional structure function  $S(\mathbf{k}, t) = \frac{1}{N} |\phi'_{\mathbf{k}}(t)|$ .  $\phi' = \tilde{\phi} - \langle \tilde{\phi} \rangle$  is the Fourier transform of the fluctuations of the order parameter  $\tilde{\phi} = \rho_r - \rho_b$ . The right plot in Fig. 5 shows the dependence of the domain size on the volume concentration of particles  $C$  for different concentrations between  $C = 0.08$  and  $C = 0.24$  for an emulsion with a fluid ratio of 1 : 1 and  $\Theta = 90^\circ$ .

The results for anisotropic particles (here:  $m = 2$ ) and spheres ( $m = 1$ ) are compared. As can be seen in the left inset of Fig. 5 these parameters for the case of  $m = 2$  lead to a bijel. For too small volume concentrations such as  $C \approx 0.04$  there are not sufficiently many particles available to stabilize the emulsion. The system finally reaches a fully demixed state. The simulation data is displayed by circles for  $m = 2$  and squares for  $m = 1$  (see [10]).  $L$  decreases with an increasing value of  $C$ . An increasing number of particles stabilizing the emulsion leads to an increase of the total interfacial area



and thus to smaller domain sizes. The results can be fitted by the equation  $L(C) = \frac{a}{C} + b$  [10] (see solid ( $m = 2$ ) and dashed ( $m = 1$ ) lines in the right plot in Fig. 5) with values  $b \approx 11.08$  for  $m = 2$  and  $b \approx 10.85$  for  $m = 1$ . The offset  $b$  is due to the finite system size in our simulation and is approximately independent of the particle shape. The factor  $a$  depends on the shape of the particles. For spheres we find a value of  $a \approx 3.86$  whereas for  $m = 2$  we find  $a \approx 2.20$ . The right plot in Fig. 5 shows that the domain size  $L$  is larger for spherical particles than for the case of anisotropic particles. If a spherical particle with a radius  $R$  and a contact angle  $\Theta = 90^\circ$  is adsorbed it reduces the interfacial area by an amount of  $A(m = 1) = 2\pi R^2$ . If an anisotropic ellipsoid with aspect ratio  $m$  and the same volume as the sphere is adsorbed and reaches the stable point (see results of the single-particle adsorption (Fig. 3(a))) the interfacial area is reduced by an amount of  $A(m) = 2\pi R_p R_o = 2\pi m^{1/3} R^2$ . For the example of  $m = 2$  we obtain a reduction of the interface area of  $A(m = 2) \approx 2\pi 1.26 R^2$ . Thus, if the particle anisotropy increases, the occupied area  $A(m)$  increases. This means that if the particle number is kept constant and the anisotropy is increased, the particles can stabilize a larger interface which leads to smaller domain sizes. As the structure of a bijel interface is quite complicated and the interfaces are generally curved it is not possible to utilize the relations given above to derive an exact dependence of the domain size  $L$  on the particle aspect ratio  $m$ . However, the qualitative difference of using spheres or ellipsoids as emulsion stabilizers can be well understood.

## 5. Conclusion and outlook

We have demonstrated simulations of anisotropic ellipsoidal particles stabilizing fluid-fluid interfaces based on a combined multicomponent lattice Boltzmann and molecular dynamics approach. We provided a description of the code implementation and its recent improvements enabling our code for efficient large-scale simulations of Pickering/bijel systems on hundreds of thousands of cores on an IBM Blue Gene/P system while sampling physical observables such as density fields or colloidal particle configurations with sufficient temporal resolution. After basic studies of adsorption trajectories for single ellipsoids we demonstrated that ellipsoidal particles can lead to a transition between bijels and Pickering emulsions depending on contact angle, particle volume concentration or fluid ratio. Further, we demonstrated that the average lateral domain size of bijels depends on the particle concentration and can be fitted by a simple  $1/C$  relation where the prefactor depends on the particle aspect ratio demonstrating that particles with  $m > 1$  are more efficient emulsion stabilizers than spheres.

## Acknowledgments

This work was financed by NWO/STW (Vidi grant of J. Harting), by the FOM/Shell IPP (09iPOG14) and within the DFG priority program “nano- and microfluidics” (SPP1264). We thank the Jülich Supercomputing Centre for the technical support and the CPU time which was allocated within a large scale grant of the Gauss Center for Supercomputing.

## References

- [1] W. Ramsden. Separation of solids in the surface-layers of solutions and ‘suspensions’. *Proc. R. Soc. Lond.*, 72:156, 1903.
- [2] S. U. Pickering. Emulsions. *J. Chem. Soc., Trans.*, 91:2001, 1907.
- [3] B. P. Binks and T. S. Horozov. *Colloid Particles at Liquid Interfaces*. Cambridge University Press, Cambridge, England, 2006.
- [4] K. Stratford, R. Adhikari, I. Pagonabarraga, J.-C. Desplat, and M. E. Cates. Colloidal jamming at interfaces: A route to fluid-bicontinuous gels. *Science*, 309:2198, 2005.

- [5] E. M. Herzig, K. A. White, A. B. Schofield, W. C. K. Poon, and P. S. Clegg. Bicontinuous emulsions stabilized solely by colloidal particles. *Nature Materials*, 6:966, 2007.
- [6] S. Succi. *The Lattice Boltzmann Equation for Fluid Dynamics and Beyond*. Numerical Mathematics and Scientific Computation. Oxford University Press, Oxford, 2001.
- [7] A. J. C. Ladd and R. Verberg. Lattice-Boltzmann simulations of particle-fluid suspensions. *J. Stat. Phys.*, 104:1191, 2001.
- [8] A. S. Joshi and Y. Sun. Multiphase lattice Boltzmann method for particle suspensions. *Phys. Rev. E*, 79:066703, 2009.
- [9] X. Shan and H. Chen. Lattice Boltzmann model for simulating flows with multiple phases and components. *Phys. Rev. E*, 47:1815, 1993.
- [10] F. Jansen and J. Harting. From Bijels to Pickering emulsions: A lattice Boltzmann study. *Phys. Rev. E*, 83:046707, 2011.
- [11] J. de Graaf, M. Dijkstra, and R. van Roij. Adsorption trajectories and free-energy separatrices for colloidal particles in contact with a liquid-liquid interface. *J. Chem. Phys.*, 132:164902, 2010.
- [12] H. Lehle, E. Noruzifar, and M. Oettel. Ellipsoidal particles at fluid interfaces. *Eur. Phys. J. E*, 26:151, 2008.
- [13] F. Bresme and J. Faraudo. Orientational transition of anisotropic nanoparticles at liquid-liquid interfaces. *J. Phys. Condens. Matter*, 19:375110, 2007.
- [14] B. Madivala, J. Fransaer, and J. Vermant. Self-assembly and rheology of ellipsoidal particles at interfaces. *Langmuir*, 25:2718, 2009.
- [15] C. K. Aidun, Y. Lu, and E.-J. Ding. Direct analysis of particulate suspensions with inertia using the discrete Boltzmann equation. *J. Fluid Mech.*, 373:287, 1998.
- [16] H. Hertz. Über die Berührung fester elastischer Körper. *Journal für die reine und angewandte Mathematik*, 92:156, 1881.
- [17] B. J. Berne and P. Pechukas. Gaussian model potentials for molecular interactions. *J. Chem. Phys.*, 56:4213, 1972.
- [18] H. Chen, B. M. Boghosian, P. V. Coveney, and M. Nekovee. A ternary lattice Boltzmann model for amphiphilic fluids. *Proc. R. Soc. Lond. A*, 456:2043, 2000.
- [19] S. Plimpton. Fast parallel algorithms for short-range molecular dynamics. *J. Comp. Phys.*, 117:1, 1995.
- [20] J. R. Clausen, D. A. Reasor Jr., and C. K. Aidun. Parallel performance of a lattice-Boltzmann/finite element cellular blood flow solver on the IBM Blue Gene/P architecture. *Comp. Phys. Comm.*, 181:1013, 2010.
- [21] A. Peters, S. Melchionna, E. Kaxiras, J. Lätt, J. Sircar, M. Bernaschi, M. Bisson, and S. Succi. Multiscale simulation of cardiovascular flows on the IBM Blue Gene/P: full heart-circulation system at near red-blood cell resolution. In: Proceedings of the 2010 ACM/IEEE International Conference for High Performance Computing, Networking, Storage and Analysis, New Orleans, LA, USA, 2010. IEEE Computer Society, p. 1.